Broadband extreme ultraviolet probing of transient gratings in vanadium dioxide

Emily Sistrunk,[1,2,8] Jakob Grilj,[1,3,8] Jaewoo Jeong,[4] Mahesh G. Samant,[4] Alexander X. Gray,[5,6] Hermann A. Dürr,[5] Stuart S. P. Parkin,[4,7] and Markus Gühr[1,*]

[1]*Stanford PULSE Institute, SLAC National Accelerator Laboratory, 2575 Sand Hill Rd., Menlo Park, California 94025, USA*

[2]*NIF and Photon Sciences, Lawrence Livermore National Laboratory, 7000 East Avenue, Livermore, California 94550, USA*

[3]*Laboratory of Ultrafast Spectroscopy, Ecole Polytechnique Federal de Lausanne, CH 1015 Switzerland*

[4]*IBM Almaden Research Center, 650 Harry Road, San Jose, California 95120, USA*

[5]*Stanford Institute for Materials and Energy Sciences, SLAC National Accelerator Laboratory, 2575 Sand Hill Rd., Menlo Park, California 94025, USA*

[6]*Department of Physics, Temple University, Philadelphia, Pennsylvania 19122, USA*

[7]*Max Planck Institute of Microstructure Physics, Halle, D 06120 Germany*

[8]*These authors contributed equally*

[*]*mguehr@stanford.edu*

Abstract: Nonlinear spectroscopy in the extreme ultraviolet (EUV) and soft x-ray spectral range offers the opportunity for element selective probing of ultrafast dynamics using core-valence transitions (Mukamel *et al.*, Acc. Chem. Res. **42**, 553 (2009)). We demonstrate a step on this path showing core-valence sensitivity in transient grating spectroscopy with EUV probing. We study the optically induced insulator-to-metal transition (IMT) of a VO_2 film with EUV diffraction from the optically excited sample. The VO_2 exhibits a change in the 3p-3d resonance of V accompanied by an acoustic response. Due to the broadband probing we are able to separate the two features.

OCIS codes: (320.7150) Ultrafast spectroscopy; (340.7480) X-rays, soft x-rays, extreme ultraviolet (EUV); (190.2055) Dynamic gratings; (320.7130) Ultrafast processes in condensed matter, including semiconductors.

References and links

1. C. La-O-Vorakiat, M. Siemens, M. M. Murnane, H. C. Kapteyn, S. Mathias, M. Aeschlimann, P. Grychtol, R. Adam, C. M. Schneider, J. M. Shaw, H. Nembach, and T. J. Silva, "Ultrafast demagnetization dynamics at the M edges of magnetic elements observed using a tabletop high-harmonic soft x-ray source," Phys. Rev. Lett. **103**(25), 257402 (2009).
2. A. Melnikov, H. Prima-Garcia, M. Lisowski, T. Giessel, R. Weber, R. Schmidt, C. Gahl, N. M. Bulgakova, U. Bovensiepen, and M. Weinelt, "Nonequilibrium magnetization dynamics of gadolinium studied by magnetic linear dichroism in time-resolved 4f core-level photoemission," Phys. Rev. Lett. **100**(10), 107202 (2008).
3. J. Vura-Weis, C.-M. Jiang, C. Liu, H. Gao, J. M. Lucas, F. M. F. de Groot, P. Yang, A. P. Alivisatos, and S. R. Leone, "Femtosecond M2,3-edge spectroscopy of transition-metal oxides: photoinduced oxidation state change in α-Fe2O3," J. Phys. Chem. Lett. **4**(21), 3667–3671 (2013).
4. Z.-H. Loh and S. R. Leone, "Capturing ultrafast quantum dynamics with femtosecond and attosecond x-ray core-level absorption spectroscopy," J. Phys. Chem. Lett. **4**(2), 292–302 (2013).
5. F. Bencivenga, S. Baroni, C. Carbone, M. Chergui, M. B. Danailov, G. D. Ninno, M. Kiskinova, L. Raimondi, C. Svetina, and C. Masciovecchio, "Nanoscale dynamics by short-wavelength four wave mixing experiments," New J. Phys. **15**(12), 123023 (2013).
6. S. Mukamel, D. Abramavicius, L. Yang, W. Zhuang, I. V. Schweigert, and D. V. Voronine, "Coherent multidimensional optical probes for electron correlations and exciton dynamics: from NMR to x-rays," Acc. Chem. Res. **42**(4), 553–562 (2009).
7. J. Stöhr, *NEXAFS Spectroscopy*. (Springer, 1996).
8. M. Martins, K. Godehusen, T. Richter, P. Wernet, and P. Zimmermann, "Open shells and multi-electron interactions: core level photoionization of the 3d metal atoms," J. Phys. At. Mol. Opt. Phys. **39**(5), R79–R125 (2006).
9. H. J. Eichler, P. Günter, and D. W. Pohl, *Laser-Induced Dynamic Gratings*. (Springer-Verlag, 1986).

#229272 - $15.00 USD Received 10 Dec 2014; revised 29 Jan 2015; accepted 1 Feb 2015; published 11 Feb 2015

10. J. Salcedo, A. Siegman, D. Dlott, and M. Fayer, "Dynamics of energy transport in molecular crystals: the picosecond transient-grating method," Phys. Rev. Lett. **41**(2), 131–134 (1978).
11. R. J. D. Miller, R. Casalegno, K. A. Nelson, and M. D. Fayer, "Laser-induced ultrasonics: A dynamic holographic approach to the measurement of weak absorptions, optoelastic constants acoustic attenuation," Chem. Phys. **72**(3), 371–379 (1982).
12. T. F. Crimmins, A. A. Maznev, and K. A. Nelson, "Transient grating measurements of picosecond acoustic pulses in metal films," Appl. Phys. Lett. **74**(9), 1344 (1999).
13. J. A. Rogers, A. A. Maznev, M. J. Banet, and K. A. Nelson, "Optical generation and characterization of acoustic waves in thin films: fundamentals and applications," Annu. Rev. Mater. Sci. **30**(1), 117–157 (2000).
14. G. D. Goodno, G. Dadusc, and R. J. D. Miller, "Ultrafast heterodyne-detected transient-grating spectroscopy using diffractive optics," J. Opt. Soc. Am. B **15**(6), 1791 (1998).
15. M. L. Cowan, J. P. Ogilvie, and R. J. D. Miller, "Two-dimensional spectroscopy using diffractive optics based phased-locked photon echoes," Chem. Phys. Lett. **386**(1-3), 184–189 (2004).
16. J. P. Ogilvie and K. J. Kubarych, "Chapter 5 Multidimensional Electronic and Vibrational Spectroscopy: An Ultrafast Probe of Molecular Relaxation and Reaction Dynamics," in *Advances In Atomic, Molecular, and Optical Physics*, vol. Volume 57, P. R. B. and C. C. L. E. Arimondo, Ed., pp. 249–321 (Academic Press, 2009).
17. R. I. Tobey, M. E. Siemens, M. M. Murnane, H. C. Kapteyn, D. H. Torchinsky, and K. A. Nelson, "Transient grating measurement of surface acoustic waves in thin metal films with extreme ultraviolet radiation," Appl. Phys. Lett. **89**(9), 091108 (2006).
18. R. I. Tobey, M. E. Siemens, O. Cohen, M. M. Murnane, H. C. Kapteyn, and K. A. Nelson, "Ultrafast extreme ultraviolet holography: dynamic monitoring of surface deformation," Opt. Lett. **32**(3), 286–288 (2007).
19. Q. Li, K. Hoogeboom-Pot, D. Nardi, M. M. Murnane, H. C. Kapteyn, M. E. Siemens, E. H. Anderson, O. Hellwig, E. Dobisz, B. Gurney, R. Yang, and K. A. Nelson, "Generation and control of ultrashort-wavelength two-dimensional surface acoustic waves at nanoscale interfaces," Phys. Rev. B **85**(19), 195431 (2012).
20. F. Morin, "Oxides which show a metal-to-insulator transition at the Neel temperature," Phys. Rev. Lett. **3**(1), 34–36 (1959).
21. Z. Yang, C. Ko, and S. Ramanathan, "Oxide electronics utilizing ultrafast metal-insulator transitions," Annu. Rev. Mater. Res. **41**(1), 337–367 (2011).
22. C. Kübler, H. Ehrke, R. Huber, R. Lopez, A. Halabica, R. F. Haglund, Jr., and A. Leitenstorfer, "Coherent structural dynamics and electronic correlations during an ultrafast insulator-to-metal phase transition in VO2," Phys. Rev. Lett. **99**(11), 116401 (2007).
23. M. Imada, A. Fujimori, and Y. Tokura, "Metal-insulator transitions," Rev. Mod. Phys. **70**(4), 1039–1263 (1998).
24. A. Cavalleri, T. Dekorsy, H. Chong, J. Kieffer, and R. Schoenlein, "Evidence for a structurally-driven insulator-to-metal transition in VO2: A view from the ultrafast timescale," Phys. Rev. B **70**(16), 161102 (2004).
25. A. Cavalleri, M. Rini, and R. W. Schoenlein, "Ultra-broadband femtosecond measurements of the photo-induced phase transition in VO_2: from the mid-IR to the hard x-rays," J. Phys. Soc. Jpn. **75**, 011004 (2006).
26. N. B. Aetukuri, A. X. Gray, M. Drouard, M. Cossale, L. Gao, A. H. Reid, R. Kukreja, H. Ohldag, C. A. Jenkins, E. Arenholz, K. P. Roche, H. A. Dürr, M. G. Samant, and S. S. P. Parkin, "Control of the metal-insulator transition in vanadium dioxide by modifying orbital occupancy," Nat. Phys. **9**(10), 661–666 (2013).
27. A. Cavalleri, M. Rini, H. H. Chong, S. Fourmaux, T. E. Glover, P. A. Heimann, J. C. Kieffer, and R. W. Schoenlein, "Band-selective measurements of electron dynamics in VO2 using femtosecond near-edge x-ray absorption," Phys. Rev. Lett. **95**(6), 067405 (2005).
28. P. Baum, D.-S. Yang, and A. H. Zewail, "4D visualization of transitional structures in phase transformations by electron diffraction," Science **318**(5851), 788–792 (2007).
29. J. Jeong, N. Aetukuri, T. Graf, T. D. Schladt, M. G. Samant, and S. S. P. Parkin, "Suppression of metal-insulator transition in VO2 by electric field-induced oxygen vacancy formation," Science **339**(6126), 1402–1405 (2013).
30. J. Grilj, E. Sistrunk, M. Koch, and M. Gühr, "A beamline for time-resolved extreme ultraviolet and soft x-ray spectroscopy," J. Anal. Bioanal. Tech. s12:005 (2014).
31. J. P. Farrell, B. K. McFarland, P. H. Bucksbaum, and M. Gühr, "Calibration of a high harmonic spectrometer by laser induced plasma emission," Opt. Express **17**(17), 15134–15144 (2009).
32. E. D. Palik, *Handbook of Optical Constants of Solids* (Academic press, 1997).
33. B. L. Henke, E. M. Gullikson, and J. C. Davis, "X-ray interactions: photoabsorption, scattering, transmission, and reflection at E = 50-30,000 eV, Z = 1-92," At. Data Nucl. Data Tables **54**(2), 181–342 (1993).
34. U. Fano, "Effects of configuration interaction on intensities and phase shifts," Phys. Rev. **124**(6), 1866–1878 (1961).
35. E. Sistrunk, J. Grilj, B. K. McFarland, J. Rohlén, A. Aguilar, and M. Gühr, "Resonant photoemission at the iron M-edge of $Fe(CO)_{5}$," J. Chem. Phys. **139**(16), 164318 (2013).
36. D. Kucharczyk and T. Niklewski, "Accurate x-ray determination of the lattice parameters and the thermal expansion coefficients of VO2 near the transition temperature," J. Appl. Cryst. **12**(4), 370–373 (1979).
37. C. N. Berglund and H. J. Guggenheim, "Electronic properties of VO2 near the semiconductor-metal transition," Phys. Rev. **185**(3), 1022–1033 (1969).
38. C. Leroux, G. Nihoul, and G. Van Tendeloo, "From VO2(B) to VO2(R): theoretical structures of VO2 polymorphs and in situ electron microscopy," Phys. Rev. B **57**(9), 5111–5121 (1998).
39. J. W. Goodman, *Introduction to Fourier Optics*, 3rd ed. (Roberts & Company, 2005).
40. F. deGroot and A. Kotani, *Core Level Spectroscopy of Solids*, (CRC Press, 2008)

#229272 - $15.00 USD Received 10 Dec 2014; revised 29 Jan 2015; accepted 1 Feb 2015; published 11 Feb 2015

1. Introduction

Ultrashort light pulses in the extreme ultraviolet (EUV) provide opportunities for element selective probing of ultrafast valence dynamics [1–4] and are even suggested for element selective multidimensional spectroscopy [5, 6]. Since core and deep valence binding energies differ strongly by element, the core to outer valence transitions are unique for different elements within one compound [7]. Prominent examples for these transitions in the EUV are the 3p-3d absorption features near the M-edge of 3d transition metals [8].

Recent time-resolved transmission spectroscopy in hematite with a broadband EUV probe continuum situated around the M-edge of iron resulted in novel insight on the charge transfer processes in metal oxides [3]. This method is sensitive to excitation induced changes of the imaginary part of the refractive index. To measure this, one has to distinguish small signal changes induced by the excitation on top of a large background. Depending on the light source noise characteristics, the background can impose a problem for obtaining sufficient signal to noise. An alternative way of measuring the sample response is based on diffracting the EUV probe from an excitation *grating*. The resulting so called transient grating (TG) spectroscopy, a special variant of the four-wave-mixing method, has been highly successful in IR and visible ultrafast spectroscopy [9–12]. The spatial refractive index modulation can be achieved by two excitation pulses that interfere on the sample under a small angle. The resulting intensity grating is transformed into an index of refraction grating by the sample. The probe pulse is then scattered off this grating, which means that the detector is free of signal without excitation pulses. TG has been utilized to examine the electronic response of complex materials, electron-phonon coupling, and molecular dynamics [12–15]. It has proven a powerful technique in chemistry and materials science, particularly in the infrared, visible and near-ultraviolet [16].

Recently the TG technique has been extended into the EUV range. The EUV probe was reflected from an excited sample to study the acoustic response of a thin metal film [17]. In this case, the grating was not present in the form of a change in refractive index but as a change in the surface height. Analyzing a small spectral band in the EUV range, it was found that the EUV, due to its short wavelength, is extremely sensitive to surface height changes, which was further applied in [17–19]. In this paper, we extend the technique and its analysis to element selective probing of an optically induced process. We use a grazing angle geometry and operate with a broad spectral bandwidth of 60% which is dispersed by the transient grating. The comparison of different parts in the spectrum allows us to study the wavelength dependent refractive index response, opening the field of element sensitive probing by EUV-TG experiments. Due to the large bandwidth we can distinguish the index of refraction response from the lattice expansion which is also present in the sample.

We demonstrate this technique for the example of vanadium dioxide (VO_2), which is a strongly-correlated material of particular interest because of a near-room-temperature thermally activated insulator-to-metal transition (IMT) [20]. The IMT can also be induced by light on an ultrafast timescale, important for ultrafast electronics applications (see for instance [21–23]). The extensive literature documents a debate over the ultrafast mechanism of the IMT in VO_2 [24–28]. The use of EUV TG spectroscopy thus allows for element selective probing of ultrafast photo-induced transitions with a table top laser source. This paper will provide a description of the transient grating beam line and typical detected signal in the experiment.

We will demonstrate the time-resolved spectral response of the VO_2 and analyze its features. We will discuss the resolution limits of the experiment and provide outlook for future improvements.

#229272 - $15.00 USD Received 10 Dec 2014; revised 29 Jan 2015; accepted 1 Feb 2015; published 11 Feb 2015

2. Method

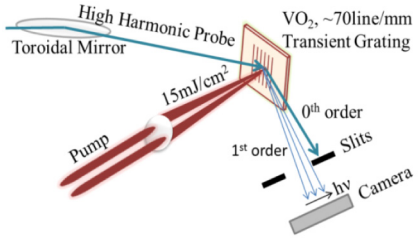

Fig. 1. Transient grating experiment geometry. A transient grating with ~15μm period is created on the VO_2 surface by two 800nm beams. High harmonics generated in a high pressure gas cell are refocused using a toroidal mirror. First order diffraction from the sample surface is detected with a CCD camera.

VO_2 films of 100nm thickness were deposited on a 0.5mm Al_2O_3 ($10\bar{1}0$) substrate by pulsed laser deposition in oxygen pressure of 10mTorr and at growth temperature of 700°C [29]. The samples were mounted in a vacuum chamber on a heated holder. The transient grating is created on the surface of the VO_2 sample by two crossing pulses of 30fs duration and of 800nm central wavelength (see Fig. 1). The grating period of ~15μm is achieved by angular separation of 4 degrees and an average fluence of 15mJ/cm^2 is created on the sample. With 30fs pulses we observe immediate sample damage for average fluence above 30mJ/cm^2 and slowly accumulated damage above 20mJ/cm^2. The EUV probe continuum is generated using high harmonic generation with a loose focusing geometry (~1.5m focal length) in an argon gas cell. It is structured in terms of odd high harmonics of the 800nm drive laser. The probe continuum is separated from the IR fundamental by a silicon wafer near Brewster angle and an aluminum filter of 150nm thickness [30]. All three beams are derived from the same 800nm, 30fs, Ti:Sapphire laser. The high harmonics are refocused with a toroidal mirror, and hit the VO_2 sample surface at a grazing angle of 22 degrees before reaching the focus at the detector. Harmonics of order 15-27 (which corresponds to photon energies of 23-42eV) are resolved in the first order diffracted signal and integrated using an EUV-sensitive back-thinned CCD camera. The CCD was typically exposed for 2.5s and binning over a 10 pixel window was performed to derive reflected spectra. For time-dependent traces each harmonic in an image was binned over a spectral width of approximately $\Delta\lambda/\lambda = 10\%$ in addition to the 10-pixel vertical binning window. The spectral calibration was performed by calculating the dispersion angle expected from the grating line spacing, which was measured independently by replacing the sample with a BBO crystal and imaging the grating pattern onto a CCD camera. Long-term drift in the source and background levels was eliminated by recording consecutive images with and without the pump beams at each time delay step. The difference images (pump on – pump off) were used in the analysis. The remaining background (mostly contributed by scattered light from the zero-order diffraction of the grating) was removed by subtracting traces integrated from detector regions vertically adjacent to each harmonic.

The delay between the grating excitation and the broadband EUV probe pulses was controlled by a translation stage using a minimum step size of 25fs which were binned in triples and summed over more than 5 time delay sweeps. The EUV pulse front sweeped with a 22 degree grazing angle across a sample region that is simultaneously pumped by the excitation pulses, which leads to a degradation of the time resolution to about 3ps. Very short lived signals will therefore be smeared out to this duration and might not become visible above the background, depending on their strength. The sample temperature was varied from 20 to 75°C to thermally induce the IMT occurring at 70° for this sample. Sample temperature stability is verified by a thermistor pressed onto the sample surface.

#229272 - $15.00 USD Received 10 Dec 2014; revised 29 Jan 2015; accepted 1 Feb 2015; published 11 Feb 2015

3. Results and discussion

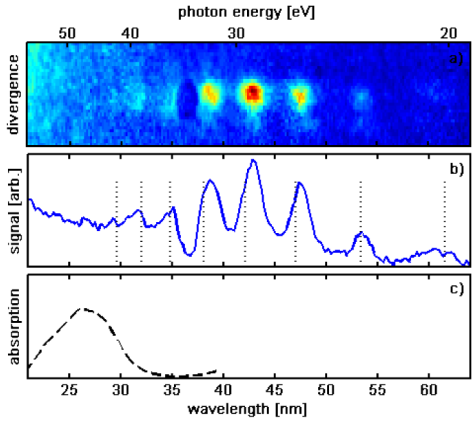

Fig. 2. Typical first order diffraction signal from VO_2. (a) Raw CCD image of 2.5s exposure on CCD camera. (b) Integrated TG spectrum from image in a. The background at short wavelength is due to diffuse scattering around the zero order. Dashed lines indicate the calculated positions of harmonic orders 13-27. (c) Absorption at V M-edge (dashed) corresponding to the 3p-3d transition, calculated from values tabulated in [33].

Figure 2(a) shows a raw image of the CCD detector for a delay of about 25 ps after grating initiation. As we show later, at such long time delays the grating is dominated by a sinusoidal amplitude variation caused by lattice expansion. The integration over the center of the image is shown in Fig. 2(b). One can clearly distinguish peaks that correspond to diffracted individual odd harmonics in the EUV probe continuum. The dashed lines indicate the harmonic positions assuming a perfect harmonic energy of the laser fundamental. Small deviations from that energy due to the intricacies of the high harmonic generation process are documented in the literature [31]. We are able to identify seven individual harmonics in the photon energy range from 20 eV to 40 eV with one acquisition setting. The reflectivity of the sample is rather high due to the grazing incidence. Due to the grazing angle, the different components of the EUV spectrum are reflected approximately equally over the wide spectral range. Under normal incidence, as implemented in [17], the reflectivity of an insulating sample typically drops by an order of magnitude over the spectral range discussed here [32].

Figure 2(c) connects the spectral range we cover with the physics of the sample. We show the calculated absorption of pure vanadium at its M-edge [33]. The index of refraction at the resonance is determined by two contributions. The first is due to valence-to-continuum transitions leading to photoionization of the sample. This contribution does not show any sharp spectral features. The second contribution is due to resonant inner-shell 3p to 3d valence transitions. Those transitions interfere with the valence-to-continuum contributions, which generally leads to the formation of so called Fano-resonances [34, 35]. For the case of VO_2, this resonance is due to transitions between the 3p band and unoccupied conduction bands having mostly vanadium 3d character.

#229272 - $15.00 USD Received 10 Dec 2014; revised 29 Jan 2015; accepted 1 Feb 2015; published 11 Feb 2015

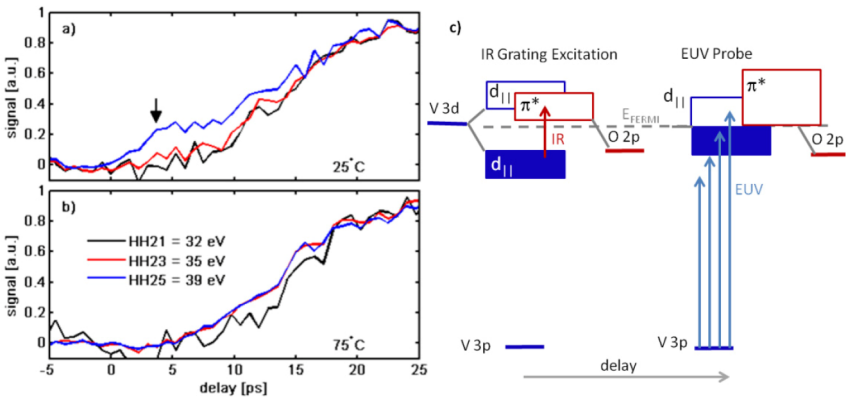

Fig. 3. Time-dependent transient grating signal as a function of photon energy and temperature. The cold sample (a) at 25°C is in the insulating phase, while the hot sample (b) at 75°C is metallic. A prompt response (marked by an arrow) of the 39 eV scattered light is only present in the cold sample. (c) Simple scheme for resonant probing showing the vanadium 3d level derived $d_{\|}$ as well as the oxygen derived π^* bands. The 3p bands are deeper bound and accessible by the extreme ultraviolet (EUV) pulses. The infrared (IR) pump pulse induced a collapse of the VO_2 bandgap, shifting the 3p-3d resonance, which is probed by a delayed EUV continuum pulse.

The time dependence of the transient response of VO_2 was studied with the sample below and above the thermally induced IMT. Time-dependent traces are included in Fig. 3 for integrated spectra at harmonic orders (HH) 21-25, corresponding to photon energies of 32 (black), 35 (red), and 39eV (blue). Those three harmonics span about 6 eV range just below the vanadium M-edge shown in Fig. 2(c). On long time-scales the diffraction shows a rise with a maximum at approximately 20ps for both room temperature (in Fig. 3(a)) and 75°C (in Fig. 3(b)) samples. The diffracted signal then decreases slowly with oscillations tens of ps in period (not shown). This long-term response is similar for all photon energies.

Examining the short term behavior, we see a marked difference in the room temperature (Fig. 3(a)) and 75°C (Fig. 3(b)) samples. For the heated phase, which is already metallic, the ultrashort pulses cannot induce the IMT. In this phase, the hot sample behaves similarly at all three photon energies. In contrast, the cold sample displays a fast-rising feature, however, only in the harmonic with 39eV photon energy. This signal increases within 3ps, much faster than the other harmonics, and then continues increasing with the same dependence as the other traces.

We first discuss the long term response of the sample. As demonstrated in Fig. 3(b) the long-term behavior of the transients shows a maximum in diffraction at approximately 20ps. *All photon energies* are modulated in a similar way. This is consistent with behavior reported from lattice dynamics in thin metal films [12, 17]. In agreement with [17], we find that the EUV diffraction is highly sensitive to thermal expansion of the sample. For the hot sample this is the result of heat deposited by the laser, while in the cold sample the mechanism includes both the lattice expansion due to laser induced heating, as well as a 0.6% contraction due to the phase transition from monoclinic to rutile due to the IMT. We estimate the expansion of the metallic sample due to absorbed laser energy to be on the order of 7Å based on the α_{33} thermal expansion coefficient [36] and reported values for the specific heat capacity [37] and density [38] of VO_2. This surface height change results in a sinusoidal phase grating, with calculated diffraction efficiency of 1% averaged over the harmonic spectral bandwidth we collect [9, 13, 39]. From the experiment we estimate a few percent diffraction efficiency, reasonably close to the calculation and in agreement with other reported diffraction efficiencies in the EUV [17].

In the short time behavior of the cold sample (in Fig. 3(a)) we notice a fast response of *only the highest energy photons,* which is absent in the hot sample. This fast response cannot

#229272 - $15.00 USD Received 10 Dec 2014; revised 29 Jan 2015; accepted 1 Feb 2015; published 11 Feb 2015

be merely the result of a surface height change because it does not affect the diffraction at the other photon energies. Therefore it must be related to a change in the index of refraction, $n(\omega)$, as a function of frequency. This demonstrates how the dispersion of a broad spectral range is crucial for separating surface change and index change.

The cause of this fast response must be the IMT because the hot, metallic sample, incapable of an optically generated IMT, does not show this fast response. In addition, the response cannot be due to a surface height change, because the different harmonics show a dramatically different response. We therefore deduce, that we observe the change of the band structure that accompanies the optically induced IMT. The low photon energies in the EUV probe spectrum are insensitive to the IMT induced changes in the band structure since they are not resonant with electronic transitions. Photons at energies below ca. 36 eV interact with the sample via ionization of the valence/conduction band into high energy continuum states. The small band changes due to the IMT result in shifts and population changes over an energy range of about 1 eV. This has a minute effect on the ionization with over 30 eV photons.

The expectations are different in the resonance region, because both the energetic position as well as the strength of the 3p-3d transition is sensitive to the exact band structure (see Fig. 3(c)). As argued in [27], the optical excitation induces holes in the $3d_{\|}$ valence band of the insulator with electrons being promoted into the mostly oxygen centered π^* band. This phenomenon alone leads to a changed refractive index in the 3p-3d resonance region. As a consequence of this excitation, the band-gap collapses on a sub-picosecond timescale leading to a shift of the resonant features to lower energies, which in turn also changes the refractive index. The optically excited stripes of the TG thus show a different refractive index compared to the non-excited stripes, which results in the diffracted signal at small time delays. We want to point out that the precise composition of the resonance spectrum is complex due to multiplet and crystal field effects [40]. Detailed simulations on how the IMT changes the TG signal must therefore be deferred to future theoretical studies. The vanadium L-edge feature in [27] decays faster than the decay observed here at 39 eV. Our transient grating signal scales with the square of the light phase shift due to the grating excitation [9]. Therefore, a rising phase change due to the acoustic response can heterodyne and thus lengthen the decaying phase change due to the IMT.

The dispersive sensitivity of the TG geometry allows us to discern resonant from nonresonant spectral features and to separate acoustic from refractive index response. Whether the energy shift of the absorption feature is due to electron correlation or changes in lattice structure is still unclear. Increased time resolution and better coverage of the entire M-edge are needed to clarify the mechanism.

4. Conclusion

This first element sensitive TG demonstrates the powerful capabilities of the method. Due to the broad bandwidth and the intrinsic dispersion of the transient grating, we succeed in separating an index of refraction change at the M edge of vanadium from the acoustic response of a VO_2 sample. The acoustic response is prominent for long time delays on the several 10 ps scale. On a shorter timescale of a few picoseconds, we find a response due to the infrared-induced IMT for cold samples. That feature is absent for hot (metallic) samples, clearly indicating its IMT character. The broadband EUV probe is sensitive to the IMT via shifting of the valence/conduction bands with respect to the inner valence 3p levels. We note that accumulated damage to the surface of the sample can create a permanent grating, producing a diffracted signal under the transient signal. This opens the interesting opportunity for future heterodyne measurements [14] allowing for signal amplification and decomposition into real and imaginary material constants.

#229272 - $15.00 USD Received 10 Dec 2014; revised 29 Jan 2015; accepted 1 Feb 2015; published 11 Feb 2015

Acknowledgments

J.G. and E.S. contributed equally to the experimental set-up, data acquisition, and analysis. J.G. acknowledges support by the European Research Agency via the FP-7 PEOPLE Program (Marie Curie Action 298210). M.G. acknowledges funding via the Office of Science Early Career Research Program through the Office of Basic Energy Sciences, U.S. Department of Energy. This work was supported by the AMOS program within the Chemical Sciences, Geosciences, and Biosciences Division of the Office of Basic Energy Sciences, Office of Science, U.S. Department of Energy. Work at SIMES was supported through the Materials Sciences and Engineering Division of the Office of Basic Energy Sciences, Office of Science, U.S. Department of Energy.

#229272 - $15.00 USD Received 10 Dec 2014; revised 29 Jan 2015; accepted 1 Feb 2015; published 11 Feb 2015